DOI: 10.31276/VJSTE.2026.0055 **Physical sciences** | *Chemistry, Engineering*

Optimisation of alkaline treatment conditions for lignocellulose enrichment from spent coffee grounds and its application in polymer composites

Quoc Vinh Ho[1, 2], Tuan Tong Tran[1, 2], Ngoc Anh Phung Thi[1, 2], Hai Nam Phan[1, 2], Hung Cuong Dinh[1, 3], Dai Hai Nguyen[1, 2], Ngoc Hoi Nguyen[1, 2*]

[1]*Institute of Advanced Technology, Vietnam Academy of Science and Technology, 1B TL29 Street, An Phu Dong Ward, Ho Chi Minh City, Vietnam*

[2]*Graduate University of Science and Technology, Vietnam Academy of Science and Technology, 18 Hoang Quoc Viet Street, Nghia Do Ward, Hanoi, Vietnam*

[3]*Sea Water Chemical Institute, Inc., 16-11 Simohata-machi, Yahatanishi-ku, Kitakyushu, Fukuoka, Japan*

Received 1 July 2026; revised 8 September 2026; accepted 29 September 2026

Abstract:

Spent coffee grounds (SCG) are promising agro-industrial residues for composite reinforcement, but non-cellulosic components limit their direct polymer application. This study evaluated the relationship between alkaline treatment parameters, the structural modifications of SCG, and its reinforcing behaviour in PVC composites. The effects of NaOH concentration, treatment time, and temperature were evaluated via single-factor experiments and optimised using response surface methodology with a Box-Behnken design. The operationally optimal conditions were identified as 4.0% NaOH, 91 min, and 62°C, yielding an experimentally validated NDF-derived lignocellulose fraction of 88.389±0.0217%. Characterisation through Fourier-transform infrared spectroscopy (FTIR), X-ray diffraction (XRD), scanning electron microscopy (SEM), and thermogravimetric analysis (TGA) confirmed the removal of non-fibrous impurities, accompanied by structural, morphological, crystalline, and thermal degradation changes. When incorporated at 40 wt.% into PVC, the treated SCG composite exhibited marked mechanical improvements, achieving compressive and flexural strengths of 79.66 and 64.03 MPa, respectively, compared with 67.80 and 38.33 MPa for the untreated SCG counterpart. Overall, optimised alkaline pretreatment provides a practical strategy to modify SCG composition and structure for value-added applications in rigid thermoplastic composites.

Keywords: **alkaline treatment, lignocellulose, mechanical properties, PVC composites, RSM optimisation, spent coffee grounds.**

Classification numbers: **2.2. 2.3**

[*]*Corresponding author: Email: hoi83bmt@gmail.com; hoi83bmt@iat.vast.vn*

1. Introduction

Coffee is one of the most frequently consumed beverages throughout the world due to its characteristic taste, specific odour, and alertness-enhancing effects [1]. According to the International Coffee Organisation (ICO), the global annual amount of coffee consumption in the 2023/2024 crop year is predicted to reach about 177.0 million bags (60 kg per bag), representing a growth of 2.2% compared to 173.1 million bags consumed last year [2]. The volume of coffee produced and exported in Vietnam, which is among the largest coffee-exporting countries around the world, is anticipated to be close to 25 million bags (or 1.5 million tonnes) for the 2023/2024 coffee crop year [3]. As coffee production continues to grow, a large amount of spent coffee grounds (SCG) is generated in the coffee industry as a major by-product [4]. Typically, there is an average production of 650 kg of wet SCG per tonne of coffee products [5]. Consequently, an estimated 6-8 million tonnes of SCG are discharged into the environment annually from the global coffee processing industry [6]. Currently, SCG waste is mainly treated using traditional methods, such as landfilling and incineration, which can lead to some negative consequences since the degradation of SCG produces substantial greenhouse gas emissions in the form of CH_4 and CO_2 that contribute to global warming [7]. In response, several valorisation pathways for SCG have been explored, including its use as fertiliser [8] and biofuel feedstock [9], and in composite materials [10] and cosmetic products [11]. However, most value-added SCG reutilisation strategies remain in the research and development stage, while the actual recycling rate remains relatively low compared with the total volume generated annually. Therefore, without effective management and utilisation, SCG may become an environmental problem; however, it can also be considered a potentially profitable biomass source for further exploitation and reuse.

According to previous studies, SCG have a polysaccharide-rich chemical composition, primarily cellulose and hemicellulose, which together account for approximately 50% of SCG dry weight [4, 12]. Specifically, the average composition of SCG includes 8-15% cellulose, 30-40% hemicellulose, and 20-30% lignin. Apart from these three main lignocellulose components, SCG also contains significant amounts of lipids (7-21%), proteins (13-17%), minerals (1-2%), and various extractive compounds [13]. Due to its diverse chemical composition, SCG has been extensively investigated for a wide range of value-added applications [14-16]. One of the promising applications for SCG is polymer composite manufacturing, as this type of raw material is known for its relatively high lignocellulose content and can act as a bio-based reinforcing phase to substitute conventional fillers [17, 18]. More broadly, bio-based composites incorporating plant-derived fibres have attracted increasing attention as alternatives to

conventional synthetic composites because of their renewable feedstocks and potential environmental benefits. Their performance is strongly influenced by the fibre characteristics, matrix selection, manufacturing process, and resulting composite structure [19]. Several research studies have focused on the incorporation of SCG into polymer matrices and the analysis of their mechanical performance and material costs [20, 21]. For instance, G. Mäder, et al. (2025) [22] utilised SCG as a filler in PBS/PBAT-based composites after drying, grinding, and particle size classification, followed by melt processing through extrusion and injection moulding at SCG loadings of 30-60%. The results showed that SCG increased material stiffness (Young's modulus) but reduced tensile strength and elongation at break. Furthermore, particle size had an important influence on mechanical behaviour, whereby smaller sizes increased ductility, and larger sizes resulted in stiffer materials. Similarly, I. Kruszelnicka, et al. (2023) [23] processed SCG through drying and fine grinding before incorporating it into HDPE at 20-40% via extrusion and injection moulding. The resulting composites exhibited increased stiffness and elastic modulus, reaching approximately 332 MPa at 40% SCG compared to 212 MPa for neat HDPE; however, impact strength decreased. In another study, N. Suaduang, et al. (2019) [24] dried, ground, and sized the raw material down to 90 µm before blending it with the matrix via twin-screw extrusion and the blown-film technique. An improvement in elongation at break was observed for all samples containing SCG; still, an opposite trend was detected for tensile strength and modulus, where tensile strength dropped from 79 to approximately 20 MPa at 10% SCG.

From the above research papers, it can be concluded that the use of SCG to reinforce polymer matrices improves certain mechanical properties and lowers the material cost; however, reinforcement efficiency remains relatively low due to insufficient filler-polymer interfacial interactions, which may be associated with the presence of lipids, proteins, and other extractive compounds [25]. In particular, such non-lignocellulose components usually occur on the lignocellulose matrix, making the surface structure heterogeneous. As a result, the heterogeneity leads to reduced compatibility between the two substances, as well as chemical and physical heterogeneity at the interface. Notably, such interfacial heterogeneity has negative implications since it decreases stress transfer efficiency and increases the tendency towards filler agglomeration and poor distribution [26, 27]. Therefore, an effective approach to remove the non-lignocellulose components is necessary to improve interfacial interactions and enhance the reinforcing effect of this biomass in the polymer matrix.

The performance of natural fibre-reinforced polymer composites is closely related to the chemical composition, structural characteristics, and surface condition of the

reinforcing phase [19, 28]. Recent research has further demonstrated the importance of surface modification for improving the performance of natural fibre-based polymer composites. For example, sodium hydroxide (NaOH) treatment of continuous sisal fibres incorporated into 3D-printed PLA composites modified the fibre surface morphology and was associated with improved mechanical performance. The treated fibre-interleaved composite exhibited higher tensile strength and interlaminar shear strength than the corresponding untreated composite, while SEM analysis of the fracture surfaces provided evidence of improved fibre-matrix adhesion [29]. These findings highlight the potential importance of fibre pretreatment in modifying the characteristics of natural lignocellulose reinforcements and improving their performance in polymer composites.

In the case of SCG, several pretreatment strategies have therefore been investigated to address the limitations associated with its heterogeneous composition and to improve its reinforcing performance in polymer composites. For instance, according to H.T.N. Kuan, et al. (2022) [30], SCG was pretreated by Soxhlet extraction in n-hexane at 80-95°C for 3 h, followed by the treatment of extracted samples with 1% NaOH solution for 24 h at room temperature prior to forming the HDPE/SCG composites through hot pressing. As a result, tensile strength increased by about 27% (up to 16.47 MPa when 10% SCG was added to the mixture), impact energy rose by approximately 16%, and water absorption was also reduced relative to raw SCG. Similar studies were conducted by P. Tapangnoi, et al. (2022) [31], where alkalisation of SCG with 5% NaOH at 70°C for 2 h followed by bleaching with $NaClO_2$ at 80°C led to the enhancement of composite hardness and modulus, as well as to an increase in tensile strength to its maximum value at approximately 10 phr of purified SCG (PSCG); however, tensile strength started to fall again at higher loadings of filler, as did elongation at break. Besides that, M.A.A. Majrashi, et al. (2024) [32] treated SCG by alkalisation with 10% NaOH for 24 h under ambient conditions, and then applied it as a reinforcing filler in PHBV composites. The maximum improvement in tensile strength (from 28.78 to 32.27 MPa), tensile modulus (up to 3.17 GPa), and flexural strength (up to 34.20 MPa) was observed at a filler content of 5%; however, all three values were lowered at 7% due to the high tendency towards filler agglomeration. Among the above-described treatment methods, alkaline treatment using NaOH is an effective approach for modifying the structure of SCG. Alkaline treatment can promote the disruption and partial removal of lignin and hemicellulose, while also facilitating the removal of non-lignocellulose components such as lipids, proteins, and other extractive organic compounds. In addition to the solubilisation of lignin and hemicellulose, alkaline treatment can induce cellulose swelling and alter the structure of the biomass, while also causing partial decrystallisation of cellulose. These changes may increase the relative

proportion of the insoluble fibre fraction. However, the effectiveness of alkaline treatment depends on several experimental parameters, particularly NaOH concentration, treatment time, and temperature. Insufficient treatment conditions may result in incomplete removal of non-lignocellulose components, whereas excessively severe conditions may cause excessive swelling, hydrolysis, and partial loss or degradation of the lignocellulose fraction. Therefore, optimisation of the treatment conditions is necessary to effectively enrich the lignocellulose fraction of SCG while minimising undesirable degradation and enhancing its potential for application in polymer composites [26, 33-35].

Despite these studies, previous investigations of alkaline-treated SCG have generally focused on applying a predetermined treatment condition and subsequently evaluating the mechanical performance of the resulting composites. The effects of individual treatment parameters have been investigated in some studies; however, the combined effects of NaOH concentration, treatment time, and temperature on the enrichment of the NDF-derived lignocellulose fraction of SCG have not been systematically optimised within a multivariate experimental framework. In addition, limited attention has been given to linking the optimised treatment conditions with the resulting physicochemical and structural modifications of SCG and subsequently evaluating their contribution to composite reinforcement. Therefore, a systematic optimisation of alkaline treatment conditions, together with characterisation of the treated material and comparative evaluation against untreated SCG in a polymer matrix, is needed to better understand the relationship between treatment conditions, material modification, and reinforcing performance. In this study, polyvinyl chloride (PVC) was selected as the polymer matrix because it is a widely used thermoplastic material in applications such as flooring, building profiles, panels, and wood-plastic composites (WPC), where relatively high filler loadings can be incorporated [36]. Therefore, PVC provides a suitable polymer system for evaluating whether the physicochemical and structural modifications of SCG induced by alkaline treatment can translate into changes in the reinforcing performance of the material. The use of SCG-derived LCell as a filler also allows the potential substitution of conventional fillers with a biomass-derived material to be investigated, thereby contributing to the value-added utilisation of SCG.

Accordingly, this study aimed to optimise the alkaline treatment of SCG by investigating the effects of NaOH concentration, treatment time, and temperature on the NDF-derived lignocellulose fraction. Following alkaline treatment, the treated SCG was designated as LCell throughout this study to distinguish it from the untreated SCG. Box-Behnken design (BBD) combined with response surface methodology (RSM) was employed to establish a multivariate model and determine the optimal combination of

treatment parameters. The optimised LCell was subsequently characterised using Fourier-transform infrared spectroscopy (FTIR), X-ray diffraction (XRD), scanning electron microscopy (SEM), and thermogravimetric analysis (TGA) to evaluate the physicochemical and structural modifications induced by alkaline treatment. Furthermore, LCell was incorporated into a PVC matrix and compared with untreated SCG in terms of compressive and flexural strength to evaluate the reinforcing effect of the alkaline treatment. This integrated approach was used to elucidate the relationship between alkaline treatment conditions, the resulting modifications of SCG, and its reinforcing performance in polymer composites.

2. Materials and methods

2.1. Materials

The SCG used in this study were collected from espresso-based coffee shops in Ho Chi Minh city, Vietnam. After collection, the SCG samples were sieved through a 1 mm mesh to remove impurities and coarse contaminants. The samples were then oven-dried at 80±2°C until the moisture content was reduced to below 5%. The dried SCG was subsequently stored in a desiccator prior to further experimental procedures.

Sodium hydroxide (NaOH, 97%), disodium hydrogen orthophosphate (Na_2HPO_4, 100%), and sodium dodecyl sulphate (SDS, 97.5%) were supplied by Fisher Scientific (the USA). Ethylenediaminetetraacetic acid disodium salt dihydrate ($C_{10}H_{18}N_2Na_2O_{10}$, 98.5%) was purchased from Sigma-Aldrich (the USA). Sodium tetraborate decahydrate ($Na_2B_4O_7.10H_2O$, 99.5%) was obtained from Xilong (China), while triethylene glycol (TEG, 99%) was supplied by Shanghai Zhanyun Chemical (China). The polymer matrix used for composite fabrication was polyvinyl chloride (PVC, SCGC, Thailand) with a K-value of 66 and a density of 0.55 g/ml. Acrylic processing aid (ACR 401) was supplied by Shandong Rike Chemical (China). Additional additives, including calcium-zinc stabiliser (Ca-Zn 518WL), polyethylene wax (PE-H100), and polyester wax (RL 1116F), were obtained from Jiangxi Hongyuan Chemical (China).

2.2. Methods

2.2.1. Chemical treatment of SCG using sodium hydroxide

The alkaline treatment conditions for SCG were investigated with respect to three primary factors: NaOH concentration (A), reaction time (B), and treatment temperature (C). The detailed experimental parameters are presented in Table 2, Table 3 and Table 4.

The experimental procedure was conducted as follows: First, 100 ml of NaOH solution was placed in a 250 ml beaker in an oil bath equipped with a magnetic stirrer. This was followed by the addition of 30 g of SCG to the mixture and stirring at 300 rpm under the required treatment conditions for each experiment. After alkaline treatment, the mixture was filtered using a cloth filter bag, and the retained solid was washed with distilled water. The solid residue was then neutralised with 1% acetic acid solution, followed by an additional washing step with distilled water until the washing liquor reached a neutral pH. Finally, the treated SCG was oven-dried at 80°C for 24 h and stored in a dry environment to prevent moisture absorption.

2.2.2. Optimisation via response surface methodology (RSM)

After determining the appropriate experimental ranges through single-factor investigations (Section 2.2.1), a Box-Behnken design (BBD) was employed to optimise the alkaline treatment parameters: NaOH concentration (A), reaction time (B), and treatment temperature (C). Three independent variables were evaluated at three coded levels (-1, 0, +1). For a three-factor BBD model, the total number of experimental runs was set to 15, including three centre points corresponding to the optimal single-factor treatment conditions identified in the preliminary experiments (Section 2.2.1). These centre points were incorporated to evaluate experimental error and assess the predictive model's reproducibility and reliability.

The relationship between the dependent variable (Y, lignocellulose content, %) and the independent variables was described using a generalised second-order polynomial regression model:

$$Y = \beta_0 + \sum_{i=1}^{k} \beta_i X_i + \sum_{i=1}^{k} \beta_{ii} X_i^2 + \sum_{i<j}^{k} \beta_{ij} X_i X_j$$

where Y is the predicted response (output); X_i, X_j are independent variables (experimental factors); β_0 is the constant coefficient (intercept); β_i is the linear coefficients; β_{ii} is the quadratic coefficients; β_{ij} is the interaction coefficients between $X_i$and X_j.

The adequacy of the model was evaluated through analysis of variance (ANOVA), including statistical parameters such as p-value, coefficient of determination (R^2), adjusted coefficient of determination (R^2_{adj}), and lack-of-fit testing to determine the degree of agreement between the predictive model and the experimental data. Regression coefficients were considered statistically significant when the p-value was <0.05.

2.2.3. Fabrication of composites

PVC, SCG, and LCell were used as the primary components for composite fabrication. SCG and LCell were sieved through a 500 μm mesh, and the fraction passing through the sieve (particle size <500 μm) was used for composite fabrication. During the experimental work, filler loadings ranging from 30 to 60 wt.% were investigated. The results indicated that a filler loading of 40 wt.% provided the most suitable balance between compressive reinforcement and retention of flexural strength within the investigated range (data not shown). Moreover, previous studies on thermoplastic composites incorporating SCG have commonly investigated filler loadings in the range of 20-40 wt.% [23, 37]. Therefore, SCG and LCell were incorporated at a fixed loading of 40 wt.% of the total composite formulation in the present study. At this relatively high filler content, the characteristics of the filler become more pronounced in terms of both mechanical reinforcement and potential adverse effects, such as filler agglomeration and property deterioration caused by poor interfacial compatibility. Comparing the two fillers at 40 wt.% therefore provides a challenging testing condition that allows the superior performance of the optimally alkali-treated LCell over raw SCG to be more clearly demonstrated, particularly in terms of improving compressive strength and mitigating the reduction in flexural strength of the composites. The amounts of the processing additives were expressed in phr (parts per hundred parts of PVC resin), where 100 parts by weight of PVC resin were used as the reference basis. Additives, including ACR, Ca/Zn thermal stabiliser, PE-H100, and RL 1116F, were incorporated to improve the processing performance and material stability of the composites. The formulation of PVC and the corresponding additives, expressed in phr, is presented in Table 1. The 40 wt.% loading of SCG or LCell refers to the filler content based on the total composite formulation and is therefore presented separately from the PVC/additive formulation in Table 1. The composite fabrication process was carried out via melt blending using a Thermo Scientific HAAKE™ Rheomex OS twin-screw extruder (the USA). The mixing zone temperature was maintained at 190°C, with a screw speed of 100 rpm and a blending time of 4.5 min. After melt compounding, the material was naturally cooled and subsequently compression-moulded into sheets using a hydraulic hot press at 190°C. Finally, the moulded samples were cooled to room temperature using a cooling system before subsequent property evaluation.

Table 1. PVC and additive composition ratios.

Components	Amount (phr)
Polyvinyl chloride (PVC)	100
Acrylic processing aid (ACR)	3.5

Ca-Zn stabiliser (Ca-Zn)	3.0
Polyester wax (RL 1116F)	1.5
Polyethylene wax (PE-H100)	0.5

2.2.4. Determination of lignocellulose content

The chemical composition of SCG was evaluated using the neutral detergent fibre (NDF) assay, which measures the insoluble fibre fraction comprising primarily cellulose, hemicellulose, and lignin. The determination of NDF in SCG was carried out according to the AOAC 2002.04 procedure described by M.B. Hall, et al. (2023) [38]. The method is based on the removal of soluble and non-fibrous components, including lipids, proteins, sugars, starches, and other soluble constituents, using a neutral detergent solution, while the insoluble fibre fraction is retained. The resulting residue is then dried and weighed to determine the NDF content. In the present study, the NDF content was used as a proxy for the lignocellulose fraction of SCG; therefore, the individual contents of cellulose, hemicellulose, and lignin were not determined separately. For clarity, the term "lignocellulose content" used throughout this study refers to the NDF content determined by the NDF assay and is used to represent the NDF-derived lignocellulose fraction of SCG.

2.2.5. Physicochemical characterisation

The FTIR spectra of the samples were recorded using a Frontier FTIR/NIR spectrometer (PerkinElmer, the USA) within the wavenumber range of 4000-400 cm^{-1} to identify functional groups.

The crystalline structure was analysed by XRD using a D8 Advance Eco diffractometer (Bruker AXS, Germany) with a Cu/Kα radiation source (λ=1.54060 Å). The samples were scanned in the 2θ range from 10 to 60° at a scanning speed of 5°/min.

The crystallinity index (CI) was calculated based on the peak intensity ratio according to the Segal method, using the following equation [39, 40]:

$$CI = \frac{I_t - I_a}{I_t} \times 100$$

where I_t is the total intensity of the (200) peak for cellulose Iβ at 2θ=22.3° or the (020) peak for cellulose II at 2θ=21.7°; I_a is the intensity of the amorphous region at 2θ=16-18° for cellulose Iβ or 2θ=12° for cellulose II.

The surface morphology was observed using field-emission scanning electron microscopy (FE-SEM, S4800, Hitachi, Japan) at an accelerating voltage of 10 kV.

The thermal degradation behaviour was evaluated using a TGA instrument (Mettler Toledo 3+, Switzerland) under a N_2 atmosphere. The samples were heated from 30 to 700°C at a constant heating rate of 10°C/min.

2.2.6. Mechanical characterisation

The mechanical properties of the composite materials were evaluated through compression testing using a Shimadzu AG-Xplus universal testing machine (20 kN) in accordance with ASTM D695. Compression test specimens were prepared with dimensions of 12.7×12.7×5.75 mm and subsequently tested under the specified standard conditions.

Three-point bending tests were performed on the same testing system in accordance with ASTM D790. Flexural specimens were prepared with dimensions of 130×15.1×5.75 mm (±0.5 mm), using a support span of 90 mm and a crosshead speed of 2.348 mm/min.

Prior to mechanical testing, all specimens were conditioned at room temperature with a relative humidity of approximately 60% for 48 h.

3. Results and discussion

3.1. Evaluation of factors affecting the insoluble fibre content

3.1.1. Effect of NaOH concentration

The effect of NaOH concentration on the lignocellulose content of LCell was investigated within the range of 2-10% (w/v) under fixed treatment conditions of 60°C and a reaction time of 120 min. The treatment time of 120 min and temperature of 60°C were selected as initial screening conditions to provide sufficient contact time and a moderate reaction temperature for the alkaline solution to interact with SCG, thereby allowing the effect of NaOH concentration to be evaluated over the investigated range. The experimental parameters and analytical results are summarised in Table 2.

Table 2. Experimental parameters and effect of NaOH concentration on the lignocellulose content of LCell.

Experiment	Code	NaOH concentration (%)	Fixed parameters	Lignocellulose content (%)
Exp 1: NaOH concentration	A2	2	Temperature: 60°C Time: 120 min	82.32^{b}±1.11
	A4	4		85.38^{a}±0.37
	A6	6		82.31^{b}±1.02
	A8	8		81.79^{b}±1.06

A10	10	81.88^{b}±1.01

[a, b]: Letters within the same column for each parameter; mean values with different superscripts are significantly different at $p<0.05$ according to Tukey's test.

The results indicate that NaOH concentration significantly influences the lignocellulose enrichment in the treated SCG. The lignocellulose content varied from 82.32 to 85.38%, with sample A4 (4% NaOH) achieving the highest lignocellulose content of 85.38±0.37%. Meanwhile, the other concentrations (2, 6, 8, and 10%) resulted in lower lignocellulose percentages, ranging from 81.79 to 82.32%.

Statistical analysis using one-way ANOVA followed by Tukey's post hoc test revealed significant differences among the treatment groups ($p<0.05$). Specifically, sample A4, labelled with the superscript "a", exhibited a statistically significant improvement in lignocellulose content compared to all other concentrations, which were labelled with the superscript "b".

At a low NaOH concentration (2%), the low availability of hydroxide ions results in insufficient disruption and solubilisation of the insoluble fibre fraction and extractive compounds present in the complex SCG structure. During alkaline treatment, NaOH dissociates into Na^{+} and OH^{-}, with hydroxide ions promoting chemical reactions that modify the biomass structure. In particular, the alkaline environment can disrupt lignin-carbohydrate linkages and promote the solubilisation or modification of susceptible components within the biomass structure. The alkaline environment can also induce swelling of the biomass structure, thereby improving the accessibility of the treatment solution to the internal components of the material. Therefore, increasing the NaOH concentration from 2 to 4% increases the availability of OH^{-}, enhancing structural disruption and the removal of susceptible non-lignocellulose components, including lipids, proteins, and other extractive organic compounds in SCG. This results in a greater relative proportion of the remaining insoluble fibre fraction and consequently increases the lignocellulose content.

However, further increasing the NaOH concentration from 4 to 6-10% resulted in a decrease in lignocellulose content. This reduction suggests that the removal of susceptible non-lignocellulose components may have been accompanied by increased interaction of NaOH with the lignocellulose fraction itself. Under stronger alkaline conditions, enhanced swelling and chemical modification of the biomass may promote the solubilisation or loss of a portion of the lignocellulose components. The maximum lignocellulose content observed at 4% NaOH therefore indicates a balance between sufficient alkaline action to remove susceptible non-lignocellulose components and excessive treatment severity that may promote the loss or degradation of the

lignocellulose fraction. Therefore, 4% NaOH was selected as the appropriate concentration for the subsequent investigation of treatment time.

3.1.2. Effect of reaction time

The effect of treatment time was investigated over a range of 30-150 min at a fixed NaOH concentration of 4% and a treatment temperature of 60°C. The experimental parameters and analytical results are presented in Table 3.

Table 3. Experimental parameters and effect of reaction time on the lignocellulose content of LCell.

Experiment	Code	Time (min)	Fixed parameters	Lignocellulose content (%)
Exp 2: Reaction time	B30	30	NaOH concentration: 4% Temperature: 60°C	81.73^{c}±0.81
	B60	60		84.53^{b}±0.97
	B90	90		88.19^{a}±0.36
	B120	120		85.38^{b}±0.37
	B150	150		84.42^{b}±0.43

$^{a, b, c}$: Letters within the same column for each parameter; mean values with different superscripts are significantly different at $p<0.05$ according to Tukey's test.

The results of the experiment showed that there was a significant impact of treatment time on the lignocellulose content of SCG when the treatment temperature and NaOH concentration remained constant at 60°C and 4%, respectively. The average lignocellulose content varied from 81.73 to 88.19%. The highest percentage of lignocellulose content was recorded in sample B90 (90 min), whereas the lowest was found in sample B30 (30 min). The treatment time of the alkaline reactions affects the structural changes in SCG. OH^- ions can promote the disruption of lignin-carbohydrate linkages, induce swelling of the biomass structure, and solubilise susceptible components. As the treatment time increases, the alkaline solution has more time to penetrate and interact with the SCG matrix, thereby promoting the removal of some chemical components and increasing the relative proportion of the insoluble fibre fraction. This was reflected by the increase in lignocellulose content from 81.73 at 30 min to 88.19% at 90 min. However, excessively prolonged treatment may increase the treatment severity, leading to the solubilisation or loss of part of the lignocellulose fraction, as indicated by the decrease to 85.38 and 84.42% at 120 and 150 min, respectively.

One-way ANOVA (single factor) analysis also proved that there was a significant difference among the treatment groups ($p<0.05$), thus indicating that the variation in treatment time had a significant impact on the lignocellulose content. Tukey's post hoc test further revealed statistically significant differences among treatment durations, as indicated by different superscript letters. Specifically, the lignocellulose content of sample B30 (superscript letter c) was significantly lower than that of all other samples, whereas sample B90 (superscript letter a) had the highest lignocellulose content and significantly differed from the intermediate treatment group. On the contrary, samples B60, B120, and B150 (superscript letter b) were not significantly different from each other ($p>0.05$). It could be concluded that the optimal treatment time was 90 minutes. Therefore, this value was taken as the fixed treatment time for subsequent experiments investigating the effect of temperature.

3.1.3. Effect of temperature

The effect of temperature was investigated over a range of 30-90°C at a fixed NaOH concentration of 4% and a reaction time of 90 min. The experimental parameters and analytical results are presented in Table 4.

Table 4. Experimental parameters and effect of temperature on the lignocellulose content of LCell.

Experiment	Code	Temperature (°C)	Fixed parameters	Lignocellulose content (%)
Exp 3: Temperature	C30	30	NaOH concentration: 4% Time: 90 minutes	86.58^{b}±0.48
	C60	60		88.19^{a}±0.36
	C90	90		85.81^{b}±0.14

[a, b]: Letters within the same column for each parameter; mean values with different superscripts are significantly different at $p<0.05$ according to Tukey's test.

The results of the experiment demonstrated that treatment temperature significantly influenced the lignocellulose content of SCG under constant conditions (4% NaOH concentration and 90 min treatment time). The mean value of the lignocellulose content ranged from 85.81 to 88.19%, with C60 (60°C) recording the highest (88.19%) and C90 (90°C) having the lowest (85.81%). The effect of temperature is mainly related to reaction rate and mass transfer during alkaline treatment. As the temperature increases, the diffusion of OH^- ions into the SCG structure may be enhanced and alkaline reactions proceed more rapidly, thereby promoting structural disruption and the removal of susceptible components. This may explain the increase in lignocellulose content from 86.58 at 30°C to 88.19% at 60°C. However, excessively

high temperatures may increase the severity of alkaline treatment, leading to excessive solubilisation or partial loss of lignocellulose components. This may explain the decrease in lignocellulose content to 85.81% at 90°C.

One-way ANOVA (single factor) showed that there were statistically significant differences between the different treatments ($p<0.05$). Therefore, treatment temperatures have a very significant effect on the lignocellulose content. Tukey's post hoc analysis indicated that there were also statistically significant differences among the individual temperatures used to treat SCG. In particular, sample C60 (superscript a) exhibited the highest value and differed significantly from samples C30 and C90 (superscript b). There were also no statistically significant differences between C30 and C90 ($p>0.05$). These findings indicate that 60°C was the optimal treatment temperature for achieving the highest lignocellulose content. Overall, the results suggest that a 4% NaOH concentration, 60°C, and 90 min are the optimal single-factor conditions for maximising lignocellulose content, achieving 88.19%.

In another study, SCG was subjected to a multistep extraction process designed to recover valuable compounds while producing cellulose-enriched material. In the first step, SCG underwent defatting via the Soxhlet technique using n-hexane as the solvent, at a solvent/material ratio of 90 ml/10 g and a temperature of 155°C for 80 min. The defatted material was later subjected to continuous flow subcritical extraction with solvents of varying polarity: 96% ethanol, 50% ethanol, and finally an aqueous phase. The last step involved treatment with 8% (w/v) NaOH at a solid/solvent ratio of 1:50 and for two cycles of 30 min each, with an extraction temperature of 115-130°C. The result shows that the NDF content increases from 58.73 in raw SCG to 81.87% in treated SCG [41].

The results indicate that the treatment conditions employed in this study (4% NaOH at 60°C for 90 min) were still effective in enriching lignocellulose content, achieving 88.19%. This is due to the disruption of lignin and hemicellulose structure, with simultaneous removal of the easily soluble constituents, such as proteins, lipids, and polyphenolic compounds.

The results showed that the selected treatment conditions in this study (4% NaOH, 60°C, and 90 min) were effective in enriching the lignocellulose content, reaching 88.19%. However, to fully evaluate the effectiveness of the treatment process, the increase in lignocellulose content should be considered together with the solid recovery. Starting with 30.0 g of SCG with an initial average lignocellulose content of 64.68%, an average of 15.84 g of treated material was recovered after treatment, washing, and drying, corresponding to a solid recovery of 52.80% and a mass loss of 47.20%. Based

on the recovered solid mass and the lignocellulose content after treatment, the actual lignocellulose recovery was approximately 72.00% of the initial lignocellulose. This indicates that the increase in lignocellulose content from 64.68 to 88.19% reflects the relative enrichment of the remaining insoluble fibre fraction after treatment, while the alkaline process also resulted in a considerable loss of solid mass, which may be associated with the removal or solubilisation of proteins, lipids, other organic compounds, and a portion of the insoluble fibre fraction during treatment.

3.2. RSM model and ANOVA analysis

Based on preliminary single-factor investigations, NaOH concentration (A), treatment time (B), and temperature (C) were identified as the principal process variables significantly affecting the lignocellulose content of SCG after alkaline treatment. Since these parameters may interact simultaneously rather than act independently, their combined effects were further systematically evaluated using design of experiments (DoE) through RSM with a Box-Behnken Design (BBD). Based on the optimal values obtained from preliminary experiments, the centre points of the BBD were established at 4% NaOH, 60°C, and 90 min. The experimental design and corresponding responses are summarised in Table 5.

Table 5. Box-Behnken experimental design and corresponding lignocellulose response values.

Run	Factor 1 (A: NaOH concentration)	Factor 2 (B: Time)	Factor 3 (C: Temperature)	Response (lignocellulose content)
	%	*min*	*°C*	*%*
1	2	60	60	83.15
2	4	60	30	84.34
3	4	60	90	85.15
4	4	90	60	88.42
5	6	60	60	83.21
6	6	90	30	83.44
7	4	90	60	88.32
8	4	90	60	88.47
9	6	90	90	83.56
10	4	120	30	84.57
11	2	90	30	83.25

12	4	120	90	84.98
13	2	90	90	83.65
14	2	120	60	83.52
15	6	120	60	83.76

Table 6 presents the ANOVA results for the quadratic Box-Behnken response surface model. The fitted model was highly significant ($F=177.04$; $p<0.0001$), supporting the adequacy of the model for describing the relationship between the treatment variables and lignocellulose content within the investigated experimental range. Furthermore, the lack-of-fit test was not statistically significant ($F=9.07$; $p=0.1009$), indicating that no significant lack of fit was detected between the model and the experimental data.

Table 6. Analysis of variance (ANOVA) results for the quadratic regression model.

Source	**Sum of squares**	**df**	**Mean square**	**F-value**	**p-value**	
Model	54.29	9	6.03	177.04	<0.0001	significant
A - NaOH concentration	0.02	1	0.02	0.587	0.4782	
B - Time	0.12	1	0.12	3.52	0.1193	
C - Temperature	0.3785	1	0.3785	11.11	0.0207	
AB	0.0081	1	0.0081	0.2377	0.6465	
AC	0.0196	1	0.0196	0.5752	0.4824	
BC	0.04	1	0.04	1.17	0.3281	
A^2	36.39	1	36.39	1067.85	<0.0001	
B^2	12.69	1	12.69	372.55	<0.0001	
C^2	11.82	1	11.82	346.88	<0.0001	
Residual	0.1704	5	0.0341			
Lack of fit	0.1587	3	0.0529	9.07	0.1009	not significant
Pure error	0.0117	2	0.0058			
Corrected total	54.46	14				

On the other hand, only temperature (C) exerted a significant effect on lignocellulose content ($p<0.05$) among the linear factors. In contrast, neither NaOH concentration (A) nor treatment time (B) had a significant influence on lignocellulose ($p>0.05$) within the investigated ranges. Regarding interactions, AB, AC, and BC were not significant ($p>0.05$). However, quadratic terms such as A^2, B^2, and C^2 were highly significant ($p<0.0001$). This indicates that lignocellulose enrichment was governed by distinct optimal treatment conditions rather than simple linear trends.

The adequacy statistics further supported the adequacy of the quadratic RSM model. The value of the R^2 was 0.9969, meaning that 99.69% of the variation in the lignocellulose content was explained by the quadratic RSM model. Moreover, the adjusted R^2 (0.9912) and predicted R^2 (0.9529) were in reasonable agreement, with a difference of 0.0383, which was less than 0.2, indicating a satisfactory predictive capability of the model. The Adequate Precision value was 34.9386, considerably higher than the desirable value of 4, indicating an adequate signal-to-noise ratio and supporting the use of the model to navigate the design space. Finally, the low standard deviation of 0.1846 and coefficient of variation of 0.2177% indicated relatively low experimental variability and good reproducibility.

The statistically significant second-order regression equation ($p<0.05$), describing the relationship between lignocellulose content (Y) and the processing variables, was expressed in both coded and actual forms as follows:

Coded equation:

$$Y = 88.40 + 0.0500*A + 0.1225*B + 0.2175*C – 3.14*A^2 – 1.85*B^2 – 1.79*C^2$$

Actual equation:

$$Y = 51.10 + 6.30333*(\text{NaOH concentration}) + 0.374917*(\text{Time}) + 0.245806*(\text{Temperature}) − 0.784792*(\text{NaOH concentration})^2 − 0.002060*(\text{Time})^2 – 0.001988*(\text{Temperature})^2$$

The regression results showed that all three process variables had effects on the lignocellulose content for the SCG treatments. The positive linear coefficients showed that increased levels of these variables led to increased lignocellulose enrichment, while negative quadratic coefficients established the nonlinear nature of the process; hence, the existence of optimum treatment levels above which there were inefficiencies. Thus, it can be seen that there exist optimum levels of operation in the alkaline treatment process, unlike the linear trends.

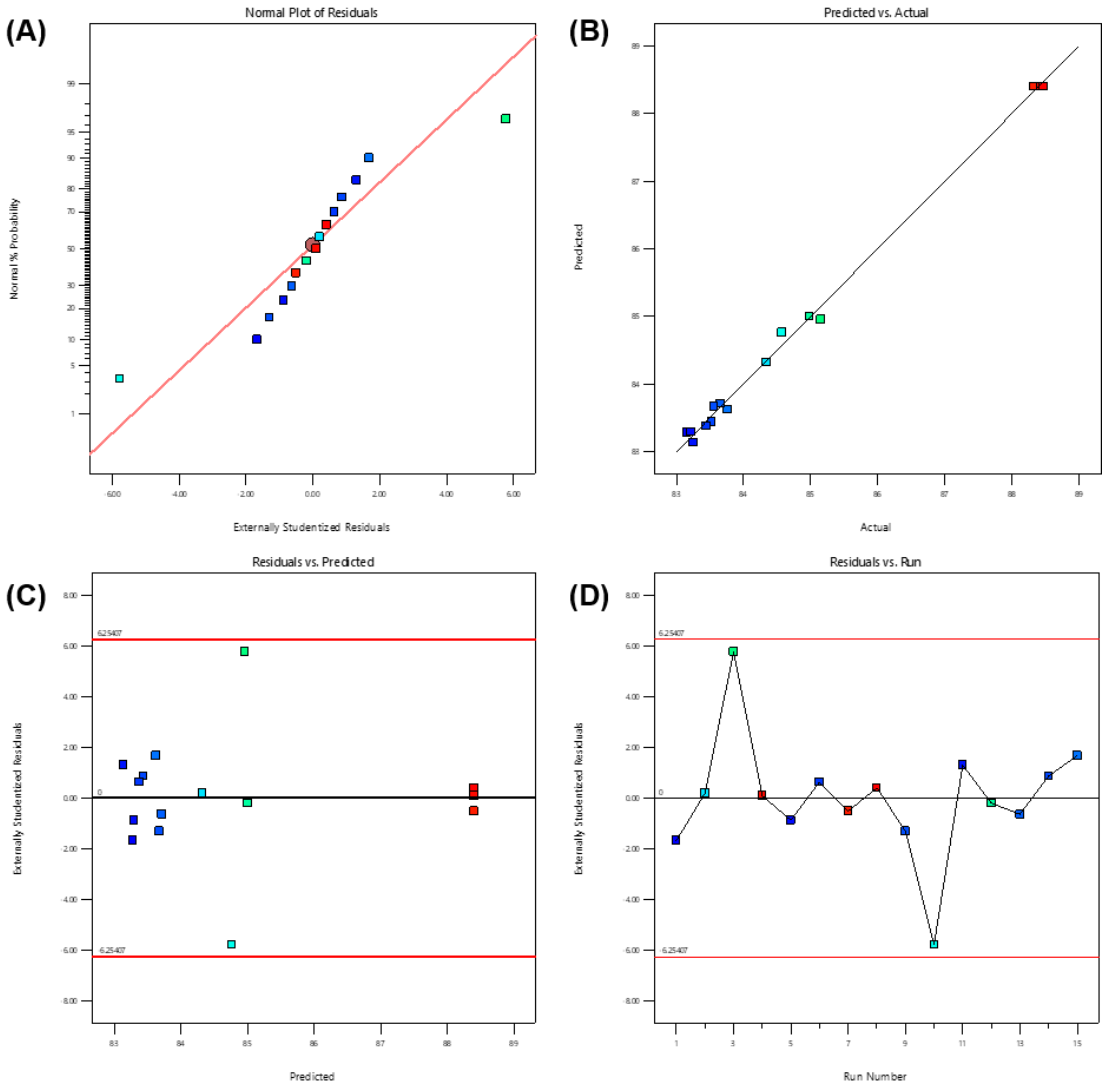


Fig. 1. Regression diagnostic plots for the Box-Behnken response surface model for the NDF-derived lignocellulose fraction of spent coffee grounds. (A) Normal probability plot of residuals; **(B)** Predicted versus actual values; **(C)** Externally studentised residuals versus predicted values; and **(D)** Externally studentised residuals versus experimental run order. Source: Made by the authors.

The regression diagnostic plots provided further support for the adequacy of the developed RSM model. The normal probability plot of residuals (Fig. 1A) showed that most of the residual points were distributed relatively close to the reference line, although some deviations were observed at the extreme values. This indicates that the residuals were reasonably consistent with the normality assumption. The predicted versus actual plot (Fig. 1B) showed that the experimental data points were closely distributed around the 45° reference line, indicating good agreement between the predicted and actual values. The externally studentised residuals versus predicted values (Fig. 1C) showed that the residuals were generally scattered around the zero line without

an apparent systematic pattern. Although two residuals approached the upper and lower diagnostic limits, both remained within the established bounds, suggesting no clear evidence of influential outliers. Similarly, the residuals versus run order plot (Fig. 1D) showed a generally random distribution around the zero line without a clear systematic trend with experimental run order, supporting the independence of the residuals. Overall, these diagnostic plots, together with the high R^2 (0.9969), adjusted R^2 (0.9912), predicted R^2 (0.9529), and adequate precision (34.9386), support the adequacy of the quadratic RSM model for describing the lignocellulose content of SCG within the investigated experimental range.

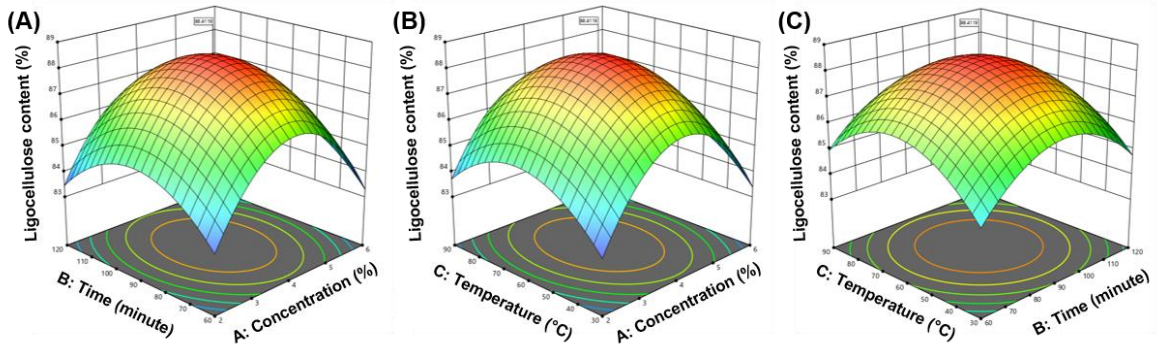


Fig. 2. Response surface plots of the RSM model for lignocellulose content showing the interactions between (A) NaOH concentration and treatment time at 61.8°C, (B) NaOH concentration and temperature at 90.975 min, and (C) treatment time and temperature at 4.016% NaOH. Source: Made by the authors.

Response surface plots (Fig. 2), which have the typical dome shape in the case of a quadratic model, show that the response variable, lignocellulose content, changed nonlinearly according to the experimental parameters. As the NaOH concentration and treatment time increased from lower to moderate levels, there was a corresponding increase in lignocellulose content; however, further increases in NaOH concentration and treatment time after moderate levels resulted in a decrease in the response surface, showing the existence of optimum regions of operation.

From the RSM numerical optimisation, the predicted optimum conditions for lignocellulose enrichment were 4.016% NaOH, 90.975 min, and 61.8°C, corresponding to a predicted lignocellulose content of 88.412% and a desirability value of 0.841. For practical experimental implementation, these values were rounded to 4.0% NaOH, 91 min, and 62°C, respectively. The validation experiment was subsequently performed under these rounded conditions using three independent replicates. The experimentally determined NDF content was 88.389±0.0217%. The percentage error between predicted and experimental values was approximately 0.026%, indicating close agreement

between the model prediction and the experimental result and supporting the predictive performance of the developed RSM model.

3.3. Characterisation of LCell in comparison with SCG

To further elucidate the structural and physicochemical modifications induced by the optimised alkaline treatment, the properties of raw SCG and LCell (SCG treated under optimal NaOH conditions) were systematically characterised and comparatively analysed using FTIR, XRD, SEM, and TGA.

3.3.1. Surface morphology via SEM analysis

SEM analysis was used to observe the surface morphology of raw SCG and treated LCell, as shown in Fig. 3. In Fig. 3A, raw SCG showed a relatively dense and uneven surface, with large block-like structures and aggregated clusters. This suggests that the lignocellulose structure appeared to be embedded in or covered by non-fibrous components present in raw SCG. At higher magnification (Fig. 3B), the SCG surface showed many adhesive patches, a rough texture, and only a few pores, indicating that non-fibrous materials were still attached to the surface.

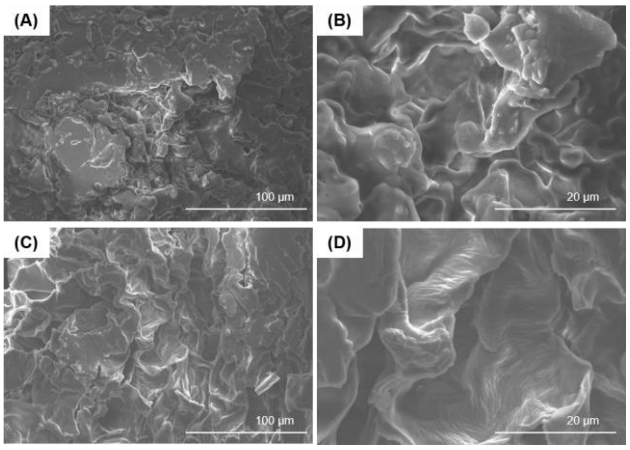


Fig. 3. SEM images of raw SCG (A, B) and treated LCell (C, D). Source: Made by the authors.

After NaOH treatment, clear changes in surface morphology were observed in LCell. In Fig. 3C, the surface became more porous, with visible holes, separated layers, grooves, and folds. At higher magnification (Fig. 3D), the cellulose fibre structure could be seen more clearly in the form of thin sheets and interwoven fibre bundles. These changes may be associated with the removal or modification of proteins, lipids, and other amorphous components during alkaline treatment, resulting in a more exposed lignocellulose structure with a more heterogeneous and porous surface morphology. The increased porosity and the observed changes in surface morphology may modify the

accessibility and surface characteristics of the treated material. From a structure-property perspective, such morphological characteristics can be relevant to the mechanical behaviour of natural fibre-reinforced composites. Recent multiscale modelling studies have emphasised that microscale features, including fibre–matrix interfacial characteristics, fibre morphology, voids, and defects, can influence stress transfer and consequently affect the macroscopic stiffness, strength, and failure behaviour of natural fibre-reinforced composites [42].

3.3.2. Fourier-transform infrared spectroscopy (FT-IR) and X-ray diffraction (XRD)

FTIR and XRD analyses were conducted to further characterise the structural and chemical properties of raw SCG and treated LCell, as shown in Fig. 4.

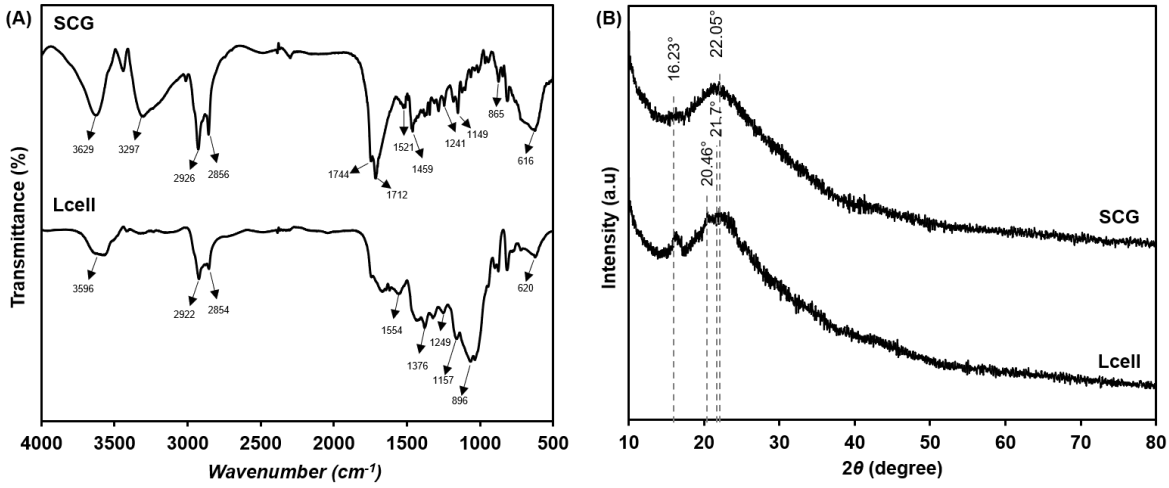


Fig. 4. FTIR spectra (A) and XRD patterns (B) of raw SCG and treated LCell samples. Source: Made by the authors.

The FTIR spectra (Fig. 4A) of raw SCG and LCell were obtained over 4000-500 cm^{-1} to evaluate the chemical structure. For raw SCG, the broad absorption peak observed at 3629-3297 cm^{-1} was assigned to O-H stretching vibrations of compounds such as cellulose, hemicellulose, and phenolics. The peaks at 2926 and 2856 cm^{-1} were attributed to asymmetric C-H stretching vibrations of aliphatic groups, like lipids and hydrocarbons. Peaks at 1744 and 1712 cm^{-1} were identified as C=O stretching vibrations of esters from triglycerides and acetyl groups of hemicellulose. Meanwhile, the absorption peak at 1521 cm^{-1} could be assigned to the aromatic ring vibrations of lignin, whereas the peaks at 1459 and 1241 cm^{-1} were identified as C-H bending and C-O-C stretching vibrations, respectively.

Following alkaline treatment, the spectrum of LCell showed several different characteristics in the bands. The disappearance of a peak around 1740 cm^{-1} suggests a reduction in ester-containing compounds, such as lipids and hemicellulose. The peaks at 2922 and 2854 cm^{-1} of the aliphatic group also had reduced intensity, related to partial removal of lipid compounds. Furthermore, the spectrum showed a change in the peak at 1554 cm^{-1}, indicating a possible reduction in protein- and phenolic-related components.

In contrast, the absorbance at 1157 cm^{-1} represented the C-O-C vibration in cellulose, while a peak at 896 cm^{-1} corresponded to the C-H bond of β-glycosidic linkages in cellulose. These enhanced peaks of cellulose (LCell sample) showed that alkaline treatment effectively removed amorphous surface components, exposing the cellulose-rich fibre structure.

The XRD patterns of raw SCG and alkali-treated LCell are presented in Fig. 4B. For raw SCG, the diffraction pattern showed a characteristic peak at $2\theta=22.05°$, corresponding to the (200) crystalline plane of cellulose I. In addition, the presence of a broad background intensity region around 16-18° indicated the existence of amorphous components associated with cellulose I [40].

After NaOH treatment, noticeable changes were observed in the diffraction pattern of LCell, reflecting structural reorganisation of the cellulose framework. The main peak at 21.7° and the smaller peak at 20.46° were attributed to the (110) and (020) planes of cellulose II, suggesting that a conversion of cellulose I to cellulose II occurred under alkaline treatment. Furthermore, these peaks are consistent with the characteristic double-peak pattern of cellulose II. However, the peak at 16.23° (cellulose I), which remained present, indicates that the phase transformation was incomplete and that both cellulose I and cellulose II coexisted within LCell. This phase transformation has also been reported in previous studies, where cellulose II is formed when native cellulose I undergoes alkalisation, followed by structural rearrangement and reorganisation of its crystalline network. Cellulose II was described as a more stable polymorphic structure with better hydrophobic associations and a denser hydrogen-bonding structure than cellulose I [43-45]. The crystallinity index (CI) also supported these findings. CI increased from 47.166 in raw SCG to 57.62% in LCell, likely because alkali treatment removed part of the amorphous material and improved the structure of the cellulose.

3.3.3. Thermal stability via TGA and DTG analysis

The thermal stability of SCG and LCell was evaluated using TGA and DTG under an inert atmosphere, as shown in Fig. 5. Both materials displayed multistep weight loss; however, notable differences in the decomposition pattern were observed after NaOH treatment, reflecting variations in their chemical composition and structure.

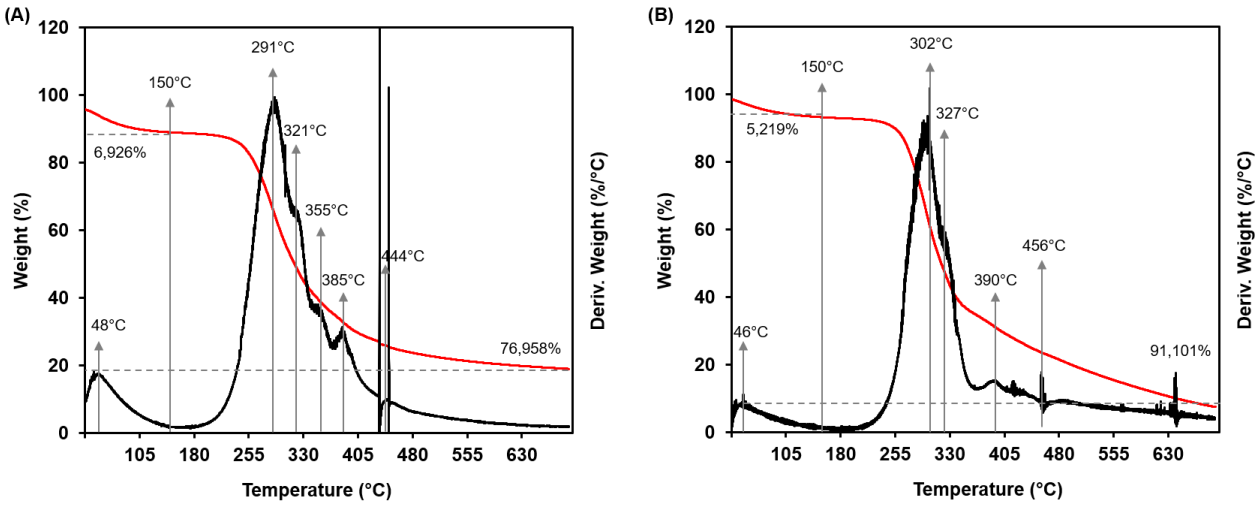


Fig. 5. TGA and DTG curves of (A) raw SCG and (B) treated LCell. Source: Made by the authors.

For raw SCG (Fig. 5A), the first stage of weight loss started below 150°C with the loss of 6.9% of mass associated with free and bound moisture. A small DTG peak accompanied this stage at around 48°C. The material was stable up to about 200°C and after that, underwent the main decomposition stage.

The primary decomposition stage of SCG occurred between 254.33 and 348.96°C with a mass loss of about 67.53%. The maximum degradation temperature (T_{max}) was recorded at around 291°C. The DTG curve showed a broad main peak with a shoulder between 330 and 360°C, which is related to the overlapping thermal decomposition of hemicellulose, cellulose, and lignin. Hemicellulose was degraded at low temperatures, whereas cellulose dominated the degradation peak. Lignin, being highly resistant to thermal degradation, caused its continuation into high-temperature ranges. Between 360 and 500°C, the SCG continued to degrade gradually, with small DTG peaks recorded at 385 and 444°C. They might be related to the degradation of lignin as well as stable components, like lipids and aromatic structures. In the final stage of thermal decomposition (500-700°C), the remaining material continued to degrade very slowly, with a char residue of about 18.93% remaining.

As shown in Fig. 5B, the thermal degradation profile of LCell showed significant differences from that of SCG after undergoing alkaline pretreatment. Firstly, the moisture loss in the first stage at temperatures below 150°C was reduced to about 5.2%. This can be explained by the removal of impurities and hydrophilic non-cellulosic components. Also, the onset temperature of the main decomposition stage increased to 266.74°C, and the final temperature decreased to 335.60°C with a total mass loss increasing to 77.39%. These changes show that the composition of LCell is more

enriched in cellulose. The DTG curve showed a dominant peak at approximately 302°C. This is typical of the thermal decomposition of cellulose, which occurs at a higher temperature than the main decomposition peak of SCG. This change indicates enhanced thermal stability because hemicellulose, lignin, and low-molecular-weight compounds are partially removed during the pretreatment process. The second peak at 327°C might be related to the decomposition of the residual hemicellulose. Further, above 350°C, there were two minor peaks at 390°C and 456°C. These are likely related to lignin degradation and other impurities. The final stage of thermal decomposition (500-700°C) for LCell showed residual ash content of only 7.43%, which is significantly lower than that of raw SCG (18.93%). This result shows that alkaline pretreatment allows for the removal of proteins, extractives, and part of the lignin, which is usually associated with char formation in the thermal decomposition process.

3.4. Mechanical properties of PVC-based composites

The mechanical properties of neat PVC, raw SCG, and PVC-based composites filled with 40 wt.% of raw SCG and LCell are illustrated in Fig. 6. It is clearly shown from the data provided that the effects of both the nature and pretreatment of the filler on mechanical performance were pronounced.

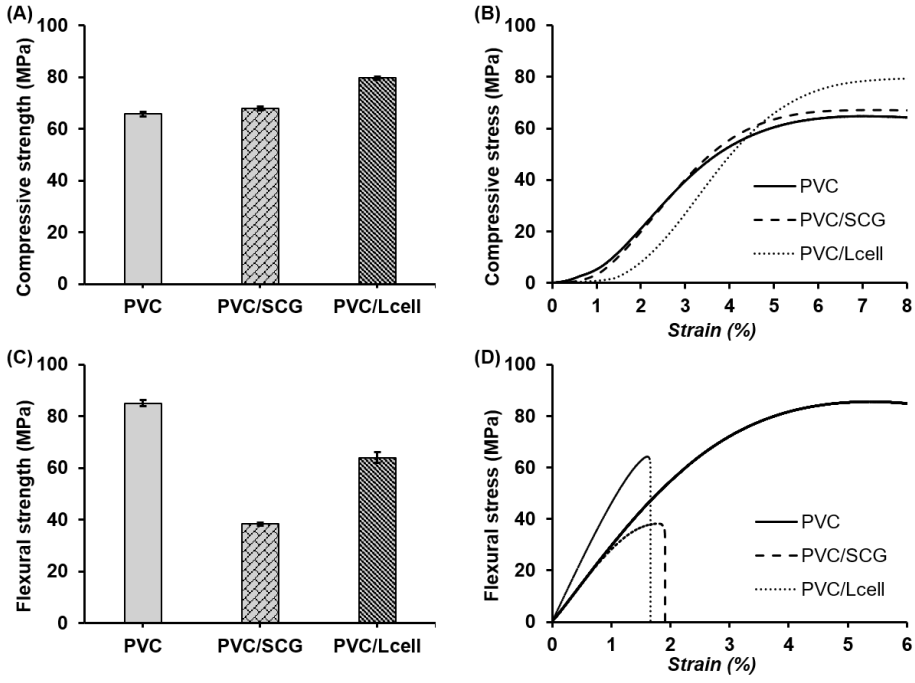


Fig. 6. Mechanical properties of PVC, PVC/SCG, and PVC/LCell composites. (A, B) Compressive strength and corresponding stress-strain curves; **(C, D)** Flexural strength and corresponding stress-strain curves. Source: Made by the authors.

For compressive strength, neat PVC demonstrated a compressive strength of around 65.73 MPa. The addition of 40 wt.% raw SCG to the polymer resulted in a slight increase in compressive strength up to 67.80 MPa due to rigid filler effects. However, it is significant that the addition of LCell as a filler played the biggest role in the compressive strength, which was equal to 79.66 MPa, outperforming neat PVC and the composite containing SCG. This improvement may be related to the physicochemical and morphological modifications induced by alkaline pretreatment, including the removal of non-fibrous and amorphous components and the exposure of a more developed lignocellulose structure.

In contrast, the flexural strength of all composite materials containing fillers decreased. First, PVC without any fillers had the highest flexural strength of 85.07 MPa. However, when the fillers were introduced into the material, the flexural strength of the material was found to decrease. Of all fillers, SCG filler caused the most substantial reduction in flexural strength in the PVC/SCG composite, which reached 38.33 MPa. The lower flexural strength of the composites may be associated with the introduction of stress concentration sites arising from limited interfacial compatibility between the filler and PVC matrix. Although the flexural strength of the PVC/LCell composite (64.03 MPa) was significantly lower than that of neat PVC, it showed a notable improvement compared to the PVC/SCG composite. Such structure-dependent effects are consistent with recent studies on natural fibre-reinforced composites, where the type, arrangement, and interfacial characteristics of the reinforcement were found to strongly influence load transfer and mechanical performance. For example, L. Techawinyutham, et al. (2026) [46] reported that the reinforcement configuration and fibre arrangement in hemp/pineapple/glass fibre composites significantly affected tensile and flexural properties, with differences in fibre-matrix bonding also reflected in the fracture morphology.

The role of reinforcement structure in determining the mechanical response of polymer composites has also been demonstrated in recent bio-based composite systems. V. Ayyappan, et al. (2025) [47] reported that the stacking sequence of jute/hemp reinforcement in a bio-epoxy matrix influenced the stiffness and viscoelastic response, with hemp-rich outer layers contributing to higher stiffness and more effective stress transfer under loading. Although the present SCG/PVC system differs from the laminated jute/hemp/bio-epoxy system in both matrix and reinforcement architecture, these findings support the broader importance of reinforcement distribution and interfacial interactions in controlling the mechanical response of natural fibre-based composites. The improved flexural performance of PVC/LCell compared with PVC/SCG may be associated with the physicochemical and morphological

modifications induced by alkaline treatment, which could improve the compatibility of LCell with the PVC matrix. Nevertheless, this improvement was insufficient to overcome the inherent incompatibility between the hydrophilic lignocellulose filler and the relatively hydrophobic PVC matrix, thereby restricting the flexibility of the material in comparison with the original plastic.

Consequently, future research should be directed towards the identification of appropriate methods for increasing the strength and flexural properties of the studied composites. For example, the use of specific chemical treatments to improve LCell-PVC interface interactions, including silane coupling agents, toughening agents, or additional compatibilisers, should be considered. Besides, adding plasticisers may prove to be efficient in improving the flexibility characteristics of developed composite materials. Additionally, it is essential to take into consideration interphase interaction and chemical compatibility while designing efficient composite materials. Furthermore, it would be useful to keep in mind other aspects that impact mechanical properties, such as filler particle size and the amount of filler used. To sum up, alkaline treatment of LCell is among the key stages in developing composite materials made of PVC and LCell with high mechanical performance and practical engineering applications.

4. Conclusions

This study demonstrates the potential of optimised alkaline treatment as an effective method for producing lignocellulose-enriched material from SCG for further composite applications. Lipid, protein, and amorphous impurity extraction significantly increases lignocellulose content without deteriorating the structure of the reinforcing matrix. Using RSM with a Box-Behnken design, the study identified the optimum conditions for maximising lignocellulose content as 4.0% NaOH, 91 min, and 62°C. Under these conditions, the experimental NDF-derived lignocellulose content reached 88.389%, showing high consistency with the model-predicted value, while achieving a lignocellulose recovery yield of approximately 72.00% of the initial lignocellulose. In terms of material evaluation, it can be observed that the process removes components that are not lignocellulose, leading to enhanced surface roughness, increased crystallinity, partial cellulose I to cellulose II polymorph conversion, and improved thermal stability. In the PVC composite application at 40 wt.% filler loading, LCell resulted in noticeable improvements in both compressive and flexural strengths compared to the untreated SCG composite. These improvements can be attributed to better physical interlocking and enhanced matrix-filler compatibility resulting from the removal of non-cellulosic surface components. Although the flexural strength of the PVC/LCell composite remained lower than that of neat PVC, its overall performance

confirms that optimised NDF-derived lignocellulose from SCG serves as a viable, eco-friendly reinforcing filler.

CRediT author statement

Quoc Vinh Ho: Conceptualisation, Methodology, Data curation, Writing - Original draft preparation, Formal analysis; Tuan Tong Tran: Formal analysis, Data curation, Visualisation; Ngoc Anh Phung Thi: Formal analysis, Software; Hai Nam Phan: Formal analysis, Data curation; Hung Cuong Dinh: Data curation, Software; Dai Hai Nguyen: Resources, Data Curation, Validation, Writing - Review & Editing; Ngoc Hoi Nguyen: Supervision, Project administration, Funding acquisition, Writing - Review & Editing.

ACKNOWLEDGEMENTS

This research was funded by the Ministry of Science and Technology of Viet Nam through the Programme for Applied Research and Development of Processing and Preservation Technologies for Agricultural, Forestry and Fishery Products and Mechanisation in Agriculture, under programme code KC.07/21-30 and project number KC.07.02/21-30.

COMPETING INTERESTS

The authors declare that they have no known competing financial interests or personal relationships that could have appeared to influence the work reported in this article.

REFERENCES

[1] L.F. Ballesteros, J.A. Teixeira, S.I. Mussatto (2014), "Chemical, functional, and structural properties of spent coffee grounds and coffee silverskin", *Food and Bioprocess Technology*, **7(12)**, pp.3493-3503, DOI: 10.1007/s11947-014-1349-z.

[2] N.M. Dilek (2025), "Utilization of spent coffee grounds as an antioxidant dietary fiber in beef patties: Oxidative stability, texture properties, and molecular docking", *Food Science & Nutrition*, **13(10)**, DOI: 10.1002/fsn3.70919.

[3] S. Ohta, D. Linh, D. Chi, et al. (2025), "Vietnam coffee market: Key updates in 2025", *B&Company World in Intelligence*, https://b-company.jp/vietnam-coffee-market-key-updates-in-2025/, accessed 26 February 2026.

[4] J. McNutt, Q. He (2019), "Spent coffee grounds: A review on current utilization", *Journal of Industrial and Engineering Chemistry*, **71**, pp.78-88, DOI: 10.1016/j.jiec.2018.11.054.

[5] J. Huang, B. Li, X. Xian, et al. (2024), "Efficient bioethanol production from spent coffee grounds using liquid hot water pretreatment without detoxification", *Fermentation*, **10**(**8**), DOI: 10.3390/fermentation10080436.

[6] E. Bevilacqua, V. Cruzat, I. Singh, et al. (2023), "The potential of spent coffee grounds in functional food development", *Nutrients*, **15(4)**, DOI: 10.3390/nu15040994.

[7] U. Choe (2025), "Valorization of spent coffee grounds and their applications in food science", *Current Research in Food Science*, **10**, DOI: 10.1016/j.crfs.2025.101010.

[8] A. Chrysargyris, O. Antoniou, P. Xylia, et al. (2020), "The use of spent coffee grounds in growing media for the production of *Brassica* seedlings in nurseries", *Environmental Science and Pollution Research*, **28(19)**, pp.24279-24290, DOI: 10.1007/s11356-020-07944-9.

[9] N.S. Caetano, V.F.M. Silva, A.C. Melo, et al. (2014), "Spent coffee grounds for biodiesel production and other applications", *Clean Technologies and Environmental Policy*, **16(7)**, pp.1423-1430, DOI: 10.1007/s10098-014-0773-0.

[10] V. Canavarro, J.L. Alves, B. Rangel (2017), "Coffee powder reused as a composite material", *Materials Design and Applications*, Springer International Publishing, pp.113-123, DOI: 10.1007/978-3-319-50784-2_9.

[11] R. Rodrigues, M.B.P.P. Oliveira, R.C. Alves (2023), "Chlorogenic acids and caffeine from coffee by-products: A review on skincare applications", *Cosmetics*, **10(1)**, DOI: 10.3390/cosmetics10010012.

[12] R. Campos-Vega, G. Loarca-Piña, H.A. Vergara-Castañeda, et al. (2015), "Spent coffee grounds: A review on current research and future prospects", *Trends in Food Science & Technology*, **45(1)**, pp.24-36, DOI: 10.1016/j.tifs.2015.04.012.

[13] A.S.C. de Bomfim, D.M. de Oliveira, E. Walling, et al. (2023), "Spent coffee grounds characterization and reuse in composting and soil amendment", *Waste*, **1(1)**, pp.2-20, DOI: 10.3390/waste1010002.

[14] A. Valencia-Isaza, M. Romero-Gámez, F. Serrano-Bernardo, et al. (2026), "Valorization of spent coffee grounds: Techno-economic and environmental assessment of a multi-product biorefinery", *Bioresource Technology*, **452**, DOI: 10.1016/j.biortech.2026.134533.

[15] J.Y. Boey, U. Kong, C.K. Lee, et al. (2024), "The effect of spent coffee ground (SCG) loading, matrix ratio and biological treatment of SCG on poly(hydroxybutyrate) (PHB)/poly(lactic acid) (PLA) polymer blend", *International Journal of Biological Macromolecules*, **266**, DOI: 10.1016/j.ijbiomac.2024.131079.

[16] K.A. Luna, C.N. Aguilar, N. Ramírez-Guzmán, et al. (2025), "Bioprocessing of spent coffee grounds as a sustainable alternative for the production of bioactive compounds", *Fermentation*, **11(7)**, DOI: 10.3390/fermentation11070366.

[17] D.K. Rajak, D.D. Pagar, P.L. Menezes, et al. (2019), "Fiber-reinforced polymer composites: Manufacturing, properties, and applications", *Polymers*, **11(10)**, DOI: 10.3390/polym11101667.

[18] H. Moustafa, C. Guizani, A. Dufresne (2017), "Sustainable biodegradable coffee grounds filler and its effect on the hydrophobicity, mechanical and thermal properties of biodegradable PBAT composites", *Journal of Applied Polymer Science*, **134(8)**, DOI: 10.1002/app.44498.

[19] G. Arora, H. Sharma, P. Bhowmik, et al. (2026b), "From plant fiber to product: Fabrication, properties, and circular pathways of bio-based composites", *Journal of Composite Materials*, DOI: 10.1177/00219983261425772.

[20] J. Tellers, P. Willems, B. Tjeerdsma, et al. (2021), "Spent coffee grounds as property enhancing filler in a wholly bio-based epoxy resin", *Macromolecular Materials and Engineering*, **306(11),** DOI: 10.1002/mame.202100323.

[21] J. Seo, L.T. Kearney, M.D. Toomey, et al. (2023), "Polyester-based epoxy vitrimer integrating spent coffee ground as a natural filler", *Composites Part B: Engineering*, **260**, DOI: 10.1016/j.compositesb.2023.110756.

[22] G. Mäder, N. Rüegg, T. Tschichold, et al. (2025), "Utilizing spent coffee grounds as sustainable fillers in biopolymer composites: Influence of particle size and content", *Sustainable Food Technology*, **3(4)**, pp.1151-1163, DOI: 10.1039/D5FB00187K.

[23] I. Kruszelnicka, M. Michałkiewicz, D. Ginter-Kramarczyk, et al. (2023), "Spent coffee as a composite filler for wastewater treatment", *Materials*, **16(3)**, DOI: 10.3390/ma16031181.

[24] N. Suaduang, S. Ross, G.M. Ross, et al. (2019), "Effect of spent coffee grounds filler on the physical and mechanical properties of poly(lactic acid) bio-composite films", *Materials Today: Proceedings*, **17**, pp.2104-2110, DOI: 10.1016/j.matpr.2019.06.260.

[25] H. Essabir, M. Raji, S.A. Laaziz, et al. (2018), "Thermo-mechanical performances of polypropylene biocomposites based on untreated, treated and compatibilized spent coffee grounds", *Composites Part B: Engineering*, **149**, pp. 1-11, DOI: 10.1016/j.compositesb.2018.05.020.

[26] M.M. Kabir, H. Wang, K.T. Lau, et al. (2012), "Chemical treatments on plant-based natural fibre reinforced polymer composites: An overview", *Composites Part B: Engineering*, **43(7)**, pp.2883-2892, DOI: 10.1016/j.compositesb.2012.04.053.

[27] A. Hasan, M.S. Rabbi, M.M. Billah (2022), "Making the lignocellulosic fibers chemically compatible for composite: A comprehensive review", *Cleaner Materials*, **4**, DOI: 10.1016/j.clema.2022.100078.

[28] J. Singh, M. Kumar, G. Arora, et al. (2026), "2 - Characteristics and properties of fiber-based natural biomaterials", *Harnessing Fiber-based Natural Biomaterials*, Woodhead Publishing, pp.33-62, DOI: 10.1016/B978-0-443-34248-6.00005-5.

[29] M. Kumar, V. Ayyappan, R. Kumar, et al. (2026), "Performance of strategically interleaved continuous sisal fiber core 3D printed PLA composites for engineering applications", *The International Journal of Advanced Manufacturing Technology*, **143(7)**, pp.3601-3616, DOI: 10.1007/s00170-026-17657-x.

[30] H.T.N. Kuan, M.Y. Tan, M.Z. Hassan, et al. (2022), "Evaluation of physico-mechanical properties on oil extracted ground coffee waste reinforced polyethylene composite", *Polymers*, **14(21)**, DOI: 10.3390/polym14214678.

[31] P. Tapangnoi, P. Sae-oui, W. Naebpetch, et al. (2022), "Preparation of purified spent coffee ground and its reinforcement in natural rubber composite", *Arabian Journal of Chemistry*, **15**, DOI: 10.1016/j.arabjc.2022.103917.

[32] M.A.A. Majrashi, R.D. Bairwan, R.Y. Mushtaq, et al. (2024), "Novel enhancement of interfacial interaction and properties in biodegradable polymer composites using green chemically treated spent coffee ground microfiller", *International Journal of Biological Macromolecules*, **266**, DOI: 10.1016/j.ijbiomac.2024.131333.

[33] V.L. Narayana, L.B. Rao (2021), "A brief review on the effect of alkali treatment on mechanical properties of various natural fiber reinforced polymer composites", *Materials Today: Proceedings*, **44**, pp.1988-1994, DOI: 10.1016/j.matpr.2020.12.117.

[34] A.E. Bekele, H.G. Lemu, M.G. Jiru (2023), "Study of the effects of alkali treatment and fiber orientation on mechanical properties of enset/sisal polymer hybrid composite", *Journal of Composites Science*, **7(1)**, DOI: 10.3390/jcs7010037.

[35] J.S. Kim, Y.Y. Lee, T.H. Kim (2016), "A review on alkaline pretreatment technology for bioconversion of lignocellulosic biomass", *Bioresource Technology*, **199**, pp.42-48, DOI: 10.1016/j.biortech.2015.08.085.

[36] D. Pervan, M. Brezović, N. Španić (2026), "Influence of reprocessing on the properties of PVC-based wood-plastic composites", *Polymers*, **18(12)**, DOI: 10.3390/polym18121509.

[37] J. Mendes, J.T. Martins, A. Manrich, et al. (2021), "Thermo-physical and mechanical characteristics of composites based on high-density polyethylene (HDPE) spent coffee grounds (SCG)", *Journal of Polymers and the Environment*, **29**, pp.1-13, DOI: 10.1007/s10924-021-02090-w.

[38] M.B. Hall, D.R. Mertens (2023), "Comparison of alternative neutral detergent fiber methods to the AOAC definitive method", *Journal of Dairy Science*, **106(8)**, pp.5364-5378, DOI: 10.3168/jds.2022-22847.

[39] S. Nam, A.D. French, B.D. Condon, et al. (2016), "Segal crystallinity index revisited by the simulation of X-ray diffraction patterns of cotton cellulose Iβ and cellulose II", *Carbohydrate Polymers*, **135**, pp.1-9, DOI: 10.1016/j.carbpol.2015.08.035.

[40] H.R. Khoshk, M. Moeenfard (2025), "TEMPO-oxidized cellulose fiber from spent coffee ground: Studying their properties as a function of particle size", *Heliyon*, **11(1)**, DOI: 10.1016/j.heliyon.2025.e41646.

[41] M. Brekalo, B.B. Rajs, K. Aladić, et al. (2023), "Multistep extraction transformation of spent coffee grounds to the cellulose-based enzyme immobilization carrier", *Sustainability*, **15(17)**, DOI: 10.3390/su151713142.

[42] G. Arora, H. Sharma, P. Bhowmik, et al. (2026b), "Recent studies on multiscale modeling of natural fiber-reinforced composites", *Archives of Computational Methods in Engineering*, **33(4)**, pp.5339-5367, DOI: 10.1007/s11831-025-10454-x.

[43] L.K. Kian, M. Jawaid, H. Ariffin, et al. (2017), "Isolation and characterization of microcrystalline cellulose from roselle fibers", *International Journal of Biological Macromolecules*, **103**, pp.931-940, DOI: 10.1016/j.ijbiomac.2017.05.135.

[44] Y. Seki (2025), "Isolation and characterization of cellulose from spent ground coffee (*Coffea arabica* L.): A comparative study", *Waste Management*, **193**, pp.54-61, DOI: 10.1016/j.wasman.2024.11.048.

[45] Y. Bouramdane, M. Haddad, A. Mazar, et al. (2024), "Aged lignocellulose fibers of cedar wood (9th and 12th century): Structural investigation using FTIR-deconvolution spectroscopy, X-ray diffraction (XRD), crystallinity indices, and morphological SEM analyses", *Polymers*, **16(23)**, DOI: 10.3390/polym16233334.

[46] L. Techawinyutham, V. Ayyappan, M. Kumar, et al. (2026), "Sustainable epoxy composites from hemp/pineapple/glass fibers for lightweight automobile panels",

International Journal of Biological Macromolecules, **337**, DOI: 10.1016/j.ijbiomac.2025.149392.

[47] V. Ayyappan, V. Raghunathan, J. Tengsuthiwat, et al. (2025), "Development of commercial fully bio-based sport utility using jute/hemp bio-epoxy composite: Influence of stacking sequence on the fatigue, thermo-mechanical, vibrational and viscoelastic behavior", *Journal of Polymer Research*, **32(6)**, DOI: 10.1007/s10965-025-04428-7.